Cancer Chemother Pharmacol (1992) 30: 355–359

Cancer Chemotherapy and Pharmacology

© Springer-Verlag 1992

Mechanism-based model for tumor drug resistance*

Thomas Kuczek[1] and Thomas C. K. Chan[2]

[1] Department of Statistics and [2] Department of Veterinary Physiology and Pharmacology, Purdue University, West Lafayette, IN 47907, USA

Received 17 October 1991/Accepted 2 March 1992

Summary. The development of tumor resistance to cytotoxic agents has important implications in the treatment of cancer. If supported by experimental data, mathematical models of resistance can provide useful information on the underlying mechanisms and aid in the design of therapeutic regimens. We report on the development of a model of tumor-growth kinetics based on the assumption that the rates of cell growth in a tumor are normally distributed. We further assumed that the growth rate of each cell is proportional to its rate of total pyrimidine synthesis (de novo plus salvage). Using an ovarian carcinoma cell line (2008) and resistant variants selected for chronic exposure to a pyrimidine antimetabolite, *N*-phosphonacetyl-L-aspartate (PALA), we derived a simple and specific analytical form describing the growth curves generated in 72 h growth assays. The model assumes that the rate of de novo pyrimidine synthesis, denoted α, is shifted down by an amount proportional to the $\log_{10}$ PALA concentration and that cells whose rate of pyrimidine synthesis falls below a critical level, denoted α_0, can no longer grow. This is described by the equation:
Probability (growth) = probability ($\alpha_0 < \alpha - \text{constant} \times \log_{10}$ [PALA]).

This model predicts that when growth curves are plotted on probit paper, they will produce straight lines. This prediction is in agreement with the data we obtained for the 2008 cells. Another prediction of this model is that the same probit plots for the resistant variants should shift to the right in a parallel fashion. Probit plots of the dose-response data obtained for each resistant 2008 line following chronic exposure to PALA again confirmed this prediction. Correlation of the rightward shift of dose responses to uridine transport ($r = 0.99$) also suggests that salvage metabolism plays a key role in tumor-cell resistance to PALA. Furthermore, the slope of the regression lines enables the detection of synergy such as that observed between dipyridamole and PALA. Although the rate-normal model was used to study the rate of salvage metabolism in PALA resistance in the present study, it may be widely applicable to modeling of other resistance mechanisms such as gene amplification of target enzymes.

Introduction

The susceptibility of a population of tumor cells to a cytotoxic treatment is typically defined as the inhibition of growth of the population in the presence of the treatment, which may also include inheritable sublethal DNA damage. This inhibition may be taken to represent some reduction in a parameter designed to measure the growth rate or it may be a measure of posttreatment cell death. An example of the former approach might be to count the number of live cells in two flasks after a specified incubation period, one being treated and the other being left untreated, assuming equal cell density prior to treatment. An example of the latter approach might be to count the number of single-cell-derived colonies formed in the presence or absence of the treatment (clonogenic assay), assuming equal initial plating density. In both cases, the measure of effectiveness can be expressed as the percentage of reduction relative to the control value.

An important aspect of the cytotoxic treatment of a population of tumor cells is often the development of *resistance* to the treatment. By resistance, we mean the ability of some target cells to proliferate as the treatment progresses. During the development of resistance, subsequent applications of the treatment are overall less effective than earlier applications. Attempts have been made to model mathematically tumor drug resistance [9] by applying the same concepts used to model bacteriophage resistance, i.e., the somatic mutation theory of Luria and Delbruck [17]. There are two problems with this line of approach to

* This work was supported by a grant from the Elsa U. Pardee Foundation

Offprint requests to: T. C. K. Chan

tumor-resistance modeling. One problem is that the fluctuation analysis underlying the theory of somatic mutation has never been successfully done in the context of drug resistance in tumor cells, although it has been attempted [16]. Another problem is that the assumption of the model that a cell is either resistant or sensitive has not been well supported by experimental data [8, 15, 18, 24, 25]. Furthermore, the prediction of this model that alternation of non-cross-resistant regimens should improve the treatment outcome has not been supported by the clinical results [18]. This indicates a problem with the assumptions of the model, which were based on a hypothetic mechanism (the occurrence of somatic mutation). Apparently, a more fruitful approach would be to base the assumptions of a model on observed mechanisms of drug action and documented modes of resistance.

In the present study, the target population was a line of human ovarian tumor cells (2008) and the treatment involved exposure to the antipyrimidine drug *N*-phosphonacetyl-L-aspartate (PALA), a potent inhibitor of aspartate transcarbamylase [10] that acts by competing with carbamoyl phosphate for the catalytic site [2]. The development of resistance to PALA was of interest to us because this drug is a very specific and potent inhibitor of *de novo* pyrimidine biosynthesis [10]. Our approach was to model both the effect of PALA on cell kinetics based on its known effect on *de novo* pyrimidine nucleotide synthesis [10] and the mechanism of resistance based on the increase in tumor salvage activity [3, 5, 11].

Heterogeneity of the rate of growth of cell populations, as evidenced by variability in the interdivisional time of individual cells has been observed in both prokaryotes and eukaryotes [12, 14, 19, 23]. Kubitschek [13] suggested that this variability could be modeled under the assumption that the growth rates of individual cells are normally distributed. He validated his model by carrying out probit analyses on several data sets of cell-generation rates. The probit plots were linear and consistent with a normal distribution of growth rates. We applied the rate-normal model of cell kinetics to 2008 cells to predict their response to the antipyrimidine drug PALA. This model was tested in both wild-type cells (not previously exposed to PALA) and resistant cells that had been chronically exposed to different concentrations of PALA.

The model assumes that the rate of de novo pyrimidine synthesis, denoted α, is directly proportional to the growth rate of individual cells and is therefore normally distributed. It also assumes that the rate of pyrimidine synthesis is reduced by an amount proportional to the logarithm of the concentration of PALA to which the cells are exposed. When a cell's rate of pyrimidine synthesis falls below a critical level, denoted α_0, cell growth is inhibited. Mathematically, these assumptions can be written as an equation:

$$\text{Probability (growth)} = \text{probability } (\alpha_0 < \alpha - K_1 \log ([\text{PALA}])), \quad (1)$$

where K_1 represents the constant of proportionality. This equation implies that cell-growth data for 2008 cells (in 72-h growth assays) form a straight line when they are plotted on probit paper.

In cells that are chronically exposed to PALA, a portion of their de novo pyrimidine synthesis is blocked. It is assumed that PALA-resistant cells augment their de novo pyrimidine synthesis by salvage activity as evidenced by their increased uridine uptake [3, 6]. This increase may be due to selective pressure and/or to a response to sublethal exposure. The dose-response curves for resistant cells therefore shift to the right by an amount proportional to the logarithm of their chronic PALA concentration. Thus, for resistant cells:

$$\text{Probability (growth)} = \text{probability } (\alpha_0 < \alpha + K_2 \log ([\text{chronic PALA}]) - K_1 \log ([\text{PALA}])), \quad (2)$$

where K_2 represents the proportionality constant for the shift. Equation 2 predicts that the magnitude of parallel shifts of the probit plots will correlate with the logarithm of chronic PALA concentration. Data collected on the 2008 cells support the models outlined by Eqs. 1 and 2.

Materials and methods

Drugs and reagents. PALA (100 mg/ml) was obtained from the Division of Cancer Treatment, National Cancer Institute (Bethesda, Md.), and dipyridamole (Persantine, 5 mg/ml) was supplied by Boehringer Ingelheim, Ltd. (Ridgefield, Conn.). All nucleosides and nucleotide standards were purchased from Sigma Chemical Co. (St. Louis, Mo.), and all other chemicals used were obtained from Fisher Scientific (Fairlawn, N.J.). All tissue-culture media and sera were purchased from Gibco (Grand Island, N.Y.).

Growth assays. Cells (2008) growing in monolayers in T-75 flasks (Falcon Plastics, Cockeysville, Md.) were harvested at 70%–80% confluence after trypsin/ethylenediaminetetraacetic acid (EDTA) treatment. They were washed twice in fresh medium and seeded at a cell concentration of 2×10^4/ml into Linbro 24-well culture plates (Flow Laboratories, McLean, Va.) containing RPMI 1640 medium plus 10% fetal bovine serum, with varying concentrations of drugs and nucleosides having been pipeted into triplicate wells. The plates were incubated in an atmosphere containing 5% CO_2 at 37° C for 72 h, and the numbers of adherent cells in each well were quantified with an electronic cell counter (Coulter Electronics, Hialeah, Fla.) after trypsinization [3].

Selection of resistant cells. In the chronic, sublethal, stepwise exposure protocol, exponentially growing 2008 cells were used in a 72-h growth assay to establish an averaged dose response to PALA ($n = 4$). The cells were then continuously exposed to 10 μM PALA in growth medium for 2 weeks. After a second growth assay to document changes in drug sensitivity, the cells were exposed to 50 μM PALA in growth medium for the next 2 weeks, with one flask of cells being continuously maintained in the 10-μM PALA medium (CS-0.01 cells). This process was repeated for media containing 100 μM (CS-0.1), 500 μM (CS-0.5), and 2 mM (CS-2) PALA until we obtained cells that could grow exponentially in 5 mM PALA (CS-5). This series of resistant cells represents a model of acquired resistance at different drug-exposure levels.

Nucleoside uptake and initial transport rates in 2008 cells. Freshly harvested cells were suspended in "uptake medium" consisting of normal RPMI 1640 medium supplemented with 10% dialyzed fetal bovine serum. [5,6-^{3}H]-Uridine (30 Ci/mM, ICN) was added to the cell suspensions to achieve a final concentration of 10 μM (10 μCi/ml), and the suspensions (5×10^6 cells in 2.0 ml) were incubated at 37° C under constant shaking. Aliquots of cells were removed at 1, 5, 10, 20, 30, and 60 min and were diluted with 10 vol. chilled PBS and then centrifuged at 4° C for 5 min at 1,000 *g*. The cell pellets were washed twice with 1 ml chilled PBS and then resuspended in 0.9 ml 0.1 M NaOH. After 10 min

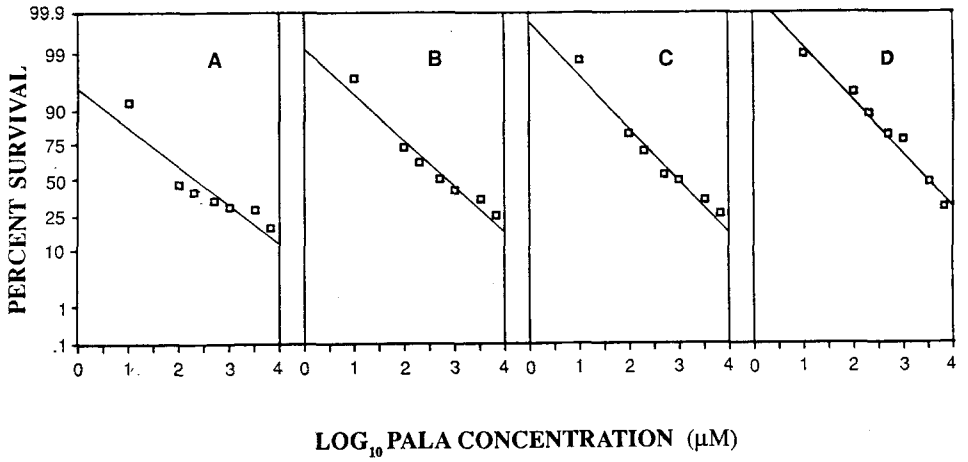

Fig. 1 A–D. Probit plots of dose responses of 2008 cells and resistant lines to log PALA concentrations. **A** 2008 wild-type cells. **B** Cells chronically exposed to 50 μM PALA. **C** Cells chronically exposed to 100 μM PALA. **D** Cells chronically exposed to 500 μM PALA. Least-squares regression lines were overlaid and the R^2 values were 0.85, 0.95, 0.97, and 0.97, respectively. Each data point represents the mean value for 4 experiments

alkaline digestion on ice, a 500-μl aliquot of each sample was removed and the radioactivity was quantified using liquid scintillation counting [3]. The intracellular radioactivity represents the amount of free radioactive uridine and its metabolites and gives estimates of the contribution of salvage metabolism in the different resistant cell types.

Uridine transport into 2008 cells was measured using a modified oil-stop method [4]. Briefly, 100 μl uptake medium containing radiolabeled uridine was carefully layered onto 100 μl of a 9:1 (v/v) mixture of silicon oil (Aldrich 17563-3) and paraffin oil (Fisher 0-119) in a 1.5-ml Eppendorf microcentrifuge tube. Transport measurements were initiated by the addition of 100 μl cell suspension, and the reactions were stopped at timed intervals of between 0 and 60 s by pelleting the cells through the oil cushion at 12,000 *g* for 30 s. The oil was then aspirated, the cell pellet was digested with 0.1 M NaOH, and the radioactivity was quantified using liquid scintillation counting. The amount of radioactivity in the cell pellet that was not associated with transport was estimated by preincubating the cells in medium containing 10 μM dipyridamole and initiating the reaction in the presence of the transport inhibitor. The intracellular radioactivity in the different resistant cells represents the contribution of the membrane nucleoside transporter (facilitated diffusion) before significant intracellular phosphorylation has taken place.

Data analysis. The normal plots were constructed as follows. The data points representing the mean percentage of cell numbers relative to control values were plotted against the $\log_{10}$ PALA concentration, with the concentration of PALA being expressed in micromolar units. The control percentage was plotted on the vertical axis and the log concentration was plotted on the horizontal axis. It should be noted that on normal or probit paper, the scale of the vertical axis is not linear for values expressed in percent; the scale for percent values is the inverse of the cumulative distribution function of the standard normal (i.e., the probit function). The computations were made using the probit function and SAS software [21], whereas the graphs were generated using the GPLOT procedure of SAS/GRAPH [20]. Statistical comparisons of the dose-response curves with respect to slopes and intercepts were made using the general linear-model procedure PROC GLM and SAS software [22]. Estimates of the drug concentration that inhibited growth by 50% (IC_{50}) and the standard deviations for the 72-h data were obtained by computation of individual IC_{50} values for each of the replications followed by calculation of the mean values and standard deviations for the wild-type cells as well as each chronically exposed line.

Results

The first prediction of the model was that both wild-type and chronically exposed 2008 cells should yield dose-response curves that produce straight lines when plotted on probit paper. In Fig. 1, 72-h growth-rate data are plotted on probit paper for the following 2008 cells: A, wild type cells; B, cells chronically exposed to 50 μM PALA; C, cells chronically exposed to 100 μM PALA; and D, cells chronically exposed to 500 μM PALA. The R^2 values for the fit of the least-squares regression lines to these data were 0.847, 0.950, 0.966, and 0.974, respectively. A statistical comparison of the slopes of the dose-response curves revealed no significant difference ($p = 0.22$), whereas a comparison of the intercepts demonstrated that they were significantly different ($p < 0.0001$) due to the rightward parallel shift of the dose-response curves for the chronically exposed 2008 cells. Table 1 lists the IC_{50} values as well as the rates of uridine transport found for the parent and resistant 2008 lines. As expected, the IC_{50} values increased as the cells were exposed on a chronic basis to increasing concentrations of PALA.

Table 1. Uridine transport rates and IC_{50} values determined for wild type and for resistant lines chronically exposed to PALA

Chronic PALA level (μM)	Transport rate[a] (pmol min^{-1} 10^{-6} cells)	IC_{50} (μM)
Wild type	16.4±2.7	224.9
50 (CS-0.05)	20.8±2.2	727.8
100 (CS-0.10)	29.2±1.8	933.3
500 (CS-0.50)	51.3±5.4	3019.9

[a] Data represent mean values ± SD for 4 experiments

Equation 2 predicted that the magnitude of parallel shifts of the probit plots would correlate with the logarithm of chronic PALA concentration. This is indeed demonstrated in Table 1 and in the left panel of Fig. 2, in which the increase in the log IC_{50} value can be seen to vary linearly with the log chronic PALA concentration ($r = 0.993$). Furthermore, the increase in uridine transport also varied linearly with the log chronic PALA concentration ($r = 0.999$) as illustrated in Table 1 and in the right panel of Fig. 2, suggesting that an increase in salvage metabolism played a major role in PALA resistance in the chronically exposed 2008 cells. Longer-term cellular uridine uptake (transport plus metabolism) paralleled the rate of transport in each of the cell lines (data not shown).

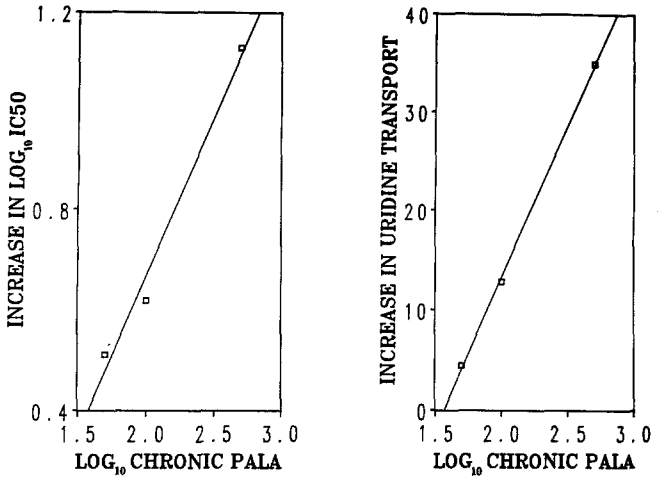

Fig. 2. Plots of increases in log IC_{50} values (*left panel*) and increases in uridine transport (*right panel*) versus log chronic PALA concentrations (μM) in the resistant lines. Each data point represents the mean value for 3 experiments, and the correlation coefficients for the plots were 0.993 and 0.999, respectively

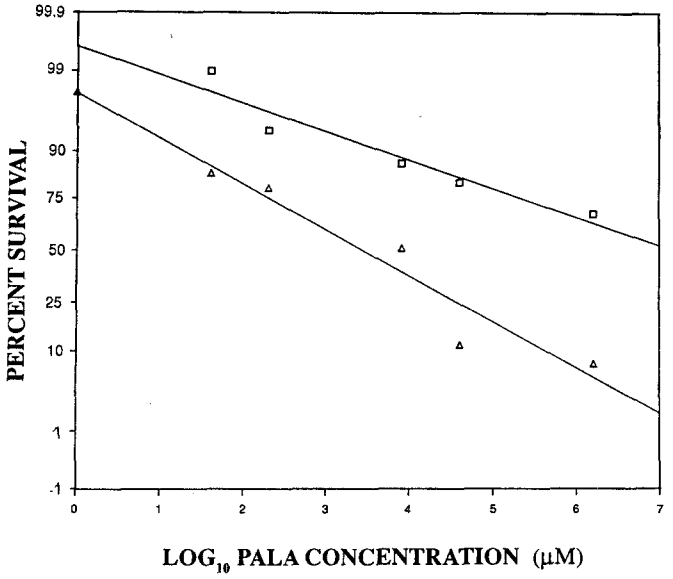

Fig. 3. Probit plots of the dose response of 2008 (wild-type) cells to PALA in the absence (□) and presence (△) of 1 μM dipyridamole. Each data point represents the mean value for 6 experiments. Least-squares regression lines were overlaid with R^2 values of 0.92 and 0.95, respectively. A comparison of the slopes indicates that the dipyridamole plus PALA line is significantly steeper ($p < 0.05$), suggesting synergy between the two drugs

In Figure 3, the dose response of 2008 cells to PALA in 72-h growth-rate assays carried out in the presence and absence of 1 μM dipyridamole are plotted on normal paper (data from Chan and Howell [3]), with least-squares regression lines being overlaid. The R^2 values for the fit of the least-squares regression lines to the data were 0.921 for PALA alone and 0.953 for PALA plus dipyridamole. This is a graphic illustration of the synergy of PALA and dipyridamole, since the slope of the dose-response curve becomes more negative in the presence of dipyridamole ($P = 0.056$).

Previous data suggest that the mechanism underlying resistance to PALA is the result of the blocked *de novo* pyrimidine synthesis being compensated by pyrimidines formed by the salvage pathway [3–5]. Dipyridamole (1 μM) is known to block uridine salvage completely by binding to a recognition protein on the cell membrane [3, 6]. In our model, we assumed that PALA induces a downshift in the mean rate of pyrimidine synthesis and that the log-normal distribution of sensitivity to PALA causes the straight lines in the probit plots. If a specific and constant amount of another drug were combined with PALA and its effect on pyrimidine synthesis were simply additive to that of PALA, the dose-response curve should shift to the left but remain parallel to the curve for PALA alone in the probit analysis. If the drug combination were synergistic, the dose-response curve for the combination would shift to the left and the slope would become steeper as shown in Fig. 3.

Discussion

We developed a mathematical model to describe the response of a population of ovarian cancer cells to the pyrimidine antimetabolite PALA. The rate-normal model enabled us to predict the specific form of the dose-response curves for normal and resistant cells in 72-h growth assays as well as the magnitude of the shift in these curves for cells that had been chronically exposed to PALA. The rate-normal model implies that when the dose-response curves are plotted on probit paper, they will form straight lines; this yields a parametric form for dose-response curves to which regression techniques may be applied for their analysis. An essential aspect of the model is that it explicitly assumes that the cell population exhibits a distribution of sensitivities to the drug. This contrasts with drug-resistance models that are based on mass action, although the two differing models can give very similar predictions (see Fig. 16 of Berenbaum [1]).

The model of tumor susceptibility and/or resistance to the pyrimidine antimetabolite PALA presented herein differs from the Goldie-Coldman model [9] in two major respects. First, it is based on observed mechanisms of drug susceptibility/resistance, whereby susceptibility is the effect of PALA in inhibiting *de novo* pyrimidine synthesis and resistance is based on the amplification of salvage activity. This model does not exclude other mechanisms of resistance such as carbamoyl-p-synthetase, aspartate, transcarboxylase, dihydronotase (CAD) gene amplification [26]. In contrast, the Goldie-Coldman model is based solely on somatic mutation, which has not been experimentally verified in tumor cell lines. Second, our model assumes that all cells are affected to some degree by the drug and that the range of susceptibility to the drug is broadly distributed among the cell population and is related to the kinetics of cell proliferation. The Goldie-Coldman model assumes that cells are either susceptible or resistant to a particular treatment and draws no finer distinctions. We do

not contend that the rate-normal model is the only model that can fit this type of data; rather, we assert that it provides a good fit and can easily be used by biomedical scientists.

Gene amplification has been documented as a mechanism of resistance to methotrexate [24, 25]. In this regard, it has been noted that the gene coding for dihydrofolate reductase, the target enzyme of methotrexate, is amplified so as to overproduce tetrahydrofolate. Some cells that are (naturally) resistant to PALA have also been found to display an amplified CAD gene [26]. In this regard, it would be desirable to relate quantitatively the rightward shift in survival curves to the increased level of gene amplification observed in chronically exposed lines, much as we related the shift in survival curves to increased uridine salvage. Gene amplification may also be involved in increased salvage activity through amplification of the gene coding for the transporter protein, although further work is required to establish this relationship.

One application of the rate-normal model involves its use to evaluate synergy in combination drug therapy. We used the model in the present study to detect the synergy between PALA and dipyridamole. This approach is consistent with but stricter than the notion that drugs are synergistic if the effect of the combination has a greater effect than the sum of the individual effects (dipyridamole has no effect by itself). The notion of synergy presented herein is also tailored for a population exhibiting a distribution of sensitivities as opposed to the isobole and median-effect notions, which are tailored for situations in which laws of mass action apply [1, 7].

Although we used rate normality to model drug resistance, it has broader applicability in the study of heterogeneous cell populations. If a population derived from a single cell displays heterogeneity, there must be a mechanism(s) for diversification that maintains the stability of the rate-normal distribution of cell kinetics in the population. This suggests an approach to the development of a theory of quantitative genetics for the study of drift and the process of selection in uniparental nondiploid populations. The drift in the rate of cell growth is the object to be modeled. The rate of cell growth is also, interestingly enough, the mechanism of selection. Beginning with a stable rate-normal model for cell kinetics, mechanisms for diversification (drift) can subsequently be tested analytically to see if they maintain this stability. We encourage other researchers to check the fit of the rate-normal model on their dose-response data sets and are prepared to provide assistance if requested.

Acknowledgements. We thank Ms. M. Janota for her excellent technical assistance and Ms. M. Epperson for her patience in preparing this manuscript.

References

1. Berenbaum MC (1989) What is synergy? Pharmacol Rev 41: 93
2. Black MJ, Jones ME (1984) Characterization and significance of carbamyl phosphate phosphatase. Cancer Res 44: 4366
3. Chan TCK, Howell SB (1985) Mechanism of synergy between *N*-phosphonacetyl-L-aspartate and dipyridamole in a human ovarian cancer line. Cancer Res 45: 3598
4. Chan TCK, Howell SB (1989) Unexpected synergy between *N*-phosphonacetyl-L-aspartate and cytidine against human tumor cells. Eur J Cancer Clin Oncol 25: 721
5. Chan TCK, Janota M (1989) The role of the membrane nucleoside transporter in natural and acquired drug resistance. Cancer Chemother Pharmacol 24 [Suppl 2]: 78
6. Chan TCK, King ME, Young B, Taetle R, Howell SB (1985) Modulation of the activity of *N*-phosphonacetyl-L-aspartate by dipyridamole. Cancer Treat Rep 69: 425
7. Chou T-C, Talalay P (1987) Applications of the median-effect principle for the assessment of low-dose risk of carcinogens and for quantitation of synergism and antagonism of chemotherapeutic agents. In: Harrip KR, Connors TA (eds) New avenues in developmental cancer chemotherapy. Academic Press, New York, p 37
8. Curt GA, Jolivet J, Carney DN, Bailey BD, Drake JC, Clendeninn NJ, Chabner BA (1985) Determinants of the sensitivity of human small cell lung cancer lines to methotrexate. J Clin Invest 76: 1323
9. Goldie JH, Coldman AJ (1979) A mathematical model for relating the drug sensitivity of tumors to their spontaneous mutation rate. Cancer Treat Rep 63: 1727
10. Grem JL, King SA, O'Dwyer PS, Leyland Jones B (1988) Biochemistry of PALA: a review. Cancer Res 48: 4441
11. Johnson RK, Swyryd EA, Stark GR (1978) Effects of *N*-(phosphonacetyl)-L-aspartate in murine tumors and normal tissues in vivo and in vitro and the relationship of sensitivity of rate of proliferation and level of aspartate transcarbamylase. Cancer Res 38: 371
12. Kelly CD, Rahn O (1932) The growth of individual bacterial cells. J Bacteriol 23: 147
13. Kubitschek H (1962) Normal distribution of cell generation rate. Exp Cell Res 26: 439
14. Kuczek T, Axelrod DE (1986) Importance of clonal heterogeneity and interexperiment variability in modeling the eukaryotic cell cycle. Math Biosci 79: 87
15. Kuczek T, Chan TCK (1988) Mathematical modeling for tumor resistance. J Natl Cancer Inst 80: 146
16. Law LW (1952) Origin of the resistance of leukemic cells to folic acid antagonists. Nature 169: 628
17. Luria SE, Delbruck M (1943) Mutations of bacteria from virus sensitivity to virus resistance. Genetics 28: 491
18. Murray N, Shah A, Wilson K, Goldie J, Voss N, Fryer C, Klimo P, Coy P, Hadzic E, Gudauskas E, Fowler R (1985) Cyclic alternating chemotherapy for small cell carcinoma of the lung. Cancer Treat Rep 69: 1241
19. Powell EO (1958) The pattern of bacterial generation times. J Gen Microbiol 18: 382
20. SAS (1985) SAS/GRAPH user's guide: basics, version 5. SAS Institute Inc., Cary, North Carolina
21. SAS (1985) SAS user's guide: basics, version 5. SAS Institute Inc., Cary, North Carolina
22. SAS (1985) SAS user's guide: statistics, version 5. SAS Institute Inc., Cary, North Carolina
23. Schaecter M, Williamson JP, Hood JR, Koch AL (1962) Growth, cell and nuclear division in some bacteria. J Gen Microbiol 29: 421
24. Schimke RT (1984) Gene amplification in cultured animal cells. Cell 37: 705
25. Schimke RT (1986) Methotrexate resistance and gene amplification: mechanisms and implications. Cancer 57: 1912
26. Stark GR, Wahl GM (1984) Gene amplification. Annu Rev Biochem 53: 447